11th International Conference
on Meson-Nucleon Physics and
the Structure of the Nucleon
September10-14, 2007
IKP, Forschungzentrum Jülich, Germany

Dynamical Coupled-Channels Model Analysis of π-N Scattering and Electromagnetic Pion Production Reactions

B. Juliá-Díaz
Departament de Estructura i Constituents de la Materia,
University of Barcelona,
Spain, 08028

Abstract

The ability of the coupled-channels model (MSL) developed in recently in Ref. [1] to account simultaneously for the πN scattering data and the π photoproduction reactions on the nucleon is presented. An accurate description of πN scattering has been obtained. A preliminary description of π photoproduction is also discussed.

1 Introduction

Understanding the intricate dynamics leading to baryon resonance production and subsequent decay is essential to deepen our understanding on the confinement mechanisms of QCD. It is now well recognized that a coupled-channels approach is needed to extract the nucleon resonance (N^*) parameters from the data of πN and electromagnetic meson production reactions. With the recent experimental developments [2,3], such a theoretical effort is needed to analyze the very extensive data from Jefferson Laboratory (JLab), Mainz, Bonn, GRAAL, and Spring-8. To cope with this challenge, a dynamical coupled-channels model (MSL) for meson-baryon reactions in the nucleon resonance region has been developed recently [1].

The details of the MSL model are given in Ref. [1] and will not be discussed here. Similar to the earlier works using meson-exchange models of pion-nucleon scattering, see Ref. [2] for a review, the starting point of the MSL model is a set of Lagrangians describing the interactions between mesons (including the photon) ($M =\gamma,\, \pi, \eta\, ,\, \rho, \omega,\, \sigma, \dots$) and baryons ($B = N, \Delta, N^*, \dots$). By applying a unitary transformation method [4,5], an effective Hamiltonian is then derived from the considered Lagrangian. All of

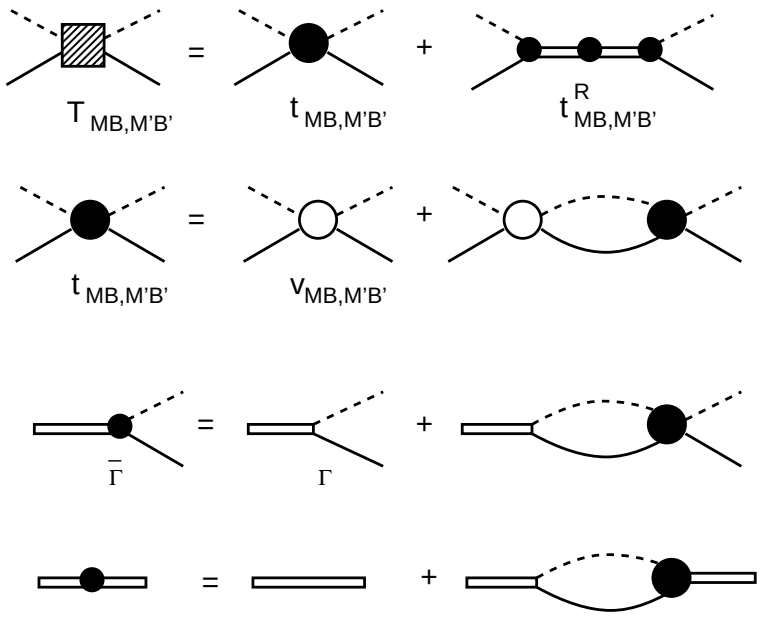

Figure 1: Graphical representation of Eqs.(1)-(8).

these interactions are *energy independent*, an important feature of the MSL formulation.

Once the Hamiltonian has been obtained, the coupled-channels equations for πN and γN reactions are derived by using the standard projection operator technique [6], as given explicitly in Ref. [1]. The obtained scattering equations satisfy the two-body ($\pi N, \eta N$, γN) and three-body ($\pi\pi N$) unitarity conditions. The $\pi\Delta$, ρN and σN resonant components of the $\pi\pi N$ continuum are generated dynamically.

The constructed model can describe up to now very well almost all of the empirical πN amplitudes in S, P, D, and F partial waves of SAID [7]. We will also show that the predicted differential cross sections and target polarization asymmetry are in good agreement with the original data of elastic $\pi^{\pm}p \to \pi^{\pm}p$ and charge-exchange $\pi^{-}p \to \pi^{0}n$ processes.

2 Dynamical coupled-channels equations

The meson-baryon (MB) scattering equations derived in Ref. [1] are illustrated in Fig. 1. Explicitly, they are defined by the following equations

$$T_{\alpha,\beta}(E) \;=\; t_{\alpha,\beta}(E) + t^{R}_{\alpha,\beta}(E)\,, \tag{1}$$

where $\alpha, \beta = \gamma N, \pi N, \eta N, \pi\pi N$. The full amplitudes, e.g. $T_{\pi N,\pi N}(E)$, $T_{\eta N,\pi N}(E)$, $T_{\pi N,\gamma N}(E)$ can be directly used to calculate πN, $\pi N \to \eta N$ and $\gamma N \to \pi N$ scattering observables. The non-resonant amplitude $t_{\alpha,\beta}(E)$ in Eq. (1) is defined by the coupled-channels equations,

$$t_{\alpha,\beta}(E) = V_{\alpha,\beta}(E) + \sum_{\delta} V_{\alpha,\delta}(E)\, G_{\delta}(E)\, t_{\delta,\beta}(E) \tag{2}$$

with

$$V_{\alpha,\beta}(E) = v_{\alpha,\beta} + Z^{(E)}_{\alpha,\beta}(E)\,. \tag{3}$$

The second term in the right-hand-side of Eq. (1) is the resonant term defined by

$$t^{R}_{\alpha,\beta}(E) = \sum_{N^*_i, N^*_j} \overline{\Gamma}_{\alpha\to N^*_i}(E)[D(E)]_{i,j}\overline{\Gamma}_{N^*_j\to\beta}(E)\,, \tag{4}$$

with

$$[D^{-1}(E)]_{i,j} = (E - M^0_{N^*_i})\delta_{i,j} - \overline{\Sigma}_{i,j}(E)\,, \tag{5}$$

where $M^0_{N^*}$ is the bare mass of the resonant state N^*, and the self-energies are

$$\overline{\Sigma}_{i,j}(E) = \sum_{\delta} \Gamma_{N^*_i\to\delta} G_{\delta}(E) \overline{\Gamma}_{\delta\to N^*_j}(E)\,. \tag{6}$$

The dressed vertex interactions in Eq. (4) and Eq. (6) are (defining $\Gamma_{\alpha\to N^*} = \Gamma^{\dagger}_{N^*\to\alpha}$)

$$\overline{\Gamma}_{\alpha\to N^*}(E) = \Gamma_{\alpha\to N^*} + \sum_{\delta} t_{\alpha,\delta}(E) G_{\delta}(E) \Gamma_{\delta\to N^*}\,, \tag{7}$$

$$\overline{\Gamma}_{N^*\to\alpha}(E) = \Gamma_{N^*\to\alpha} + \sum_{\delta} \Gamma_{N^*\to\delta} G_{\delta}(E) t_{\delta,\alpha}(E)\,. \tag{8}$$

3 Meson-baryon interaction

We proceed in the following way. First we consider the meson-baryon interactions involving $\pi N, \eta N, (\pi\Delta, \sigma N, \rho N)$ and use the extensive database for $\pi N \to \pi N$ (and also the $\pi N \to \eta N$) to fix the non-resonant parameters entering in the phenomenological lagrangians. Once the meson-baryon is fixed we will, in a first stage, leave it unchanged and produce a first description of

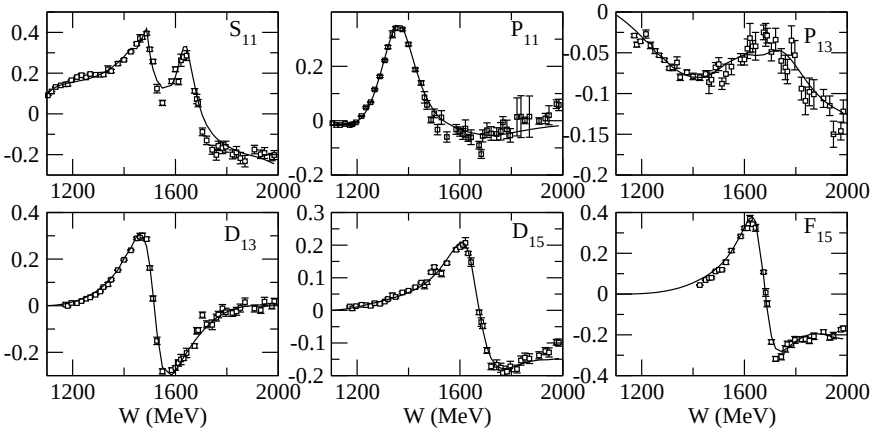

Figure 2: Real part of $T_{\pi N,\pi N}$ for some isospin 1/2 partial waves compared to the SAID energy independent extraction.

the single meson photoproduction data. In the next step a combined analysis will need to be performed.

To solve the coupled-channels integral equations, Eq. (2), without introducing any further simplification we need to regularize the matrix elements of $v_{MB,M'B'}$. We include at each meson-baryon-baryon vertex a form factor of the following form

$$F(\vec{k},\Lambda) = \left[\frac{|\vec{k}|^2}{|\vec{k}|^2+\Lambda^2}\right]^2 \tag{9}$$

ith $\vec{k}$ being the meson momentum. For the meson-meson-meson the same form is used with $\vec{k}$ being the momentum of the exchanged meson.

With the non-resonant amplitudes generated from solving Eq. (2), the resonant amplitude $t^R_{MB,M'B'}$ Eq. (4) then depends on the bare mass $M^0_{N^*}$ and the bare $N^* \to MB$ vertex functions. It is worth recalling that the resonance amplitude will necessarily contain information about the non-resonant piece, as is apparent from Eq. (4). As discussed in Ref. [1], these bare N^* parameters can perhaps be taken from a hadron structure calculation which *does not* include coupling with meson-baryon continuum states or meson-exchange quark interactions. Unfortunately, such information is not available to us. We thus use a parameterization given explicitly in Ref. [8].

In figures 2 and 3 we depict the real and imaginary part of $T_{\pi N,\pi N}$ matrix compared to the energy independent extraction of the GWU group [7]. A comparison with experimental data for differential cross section and target

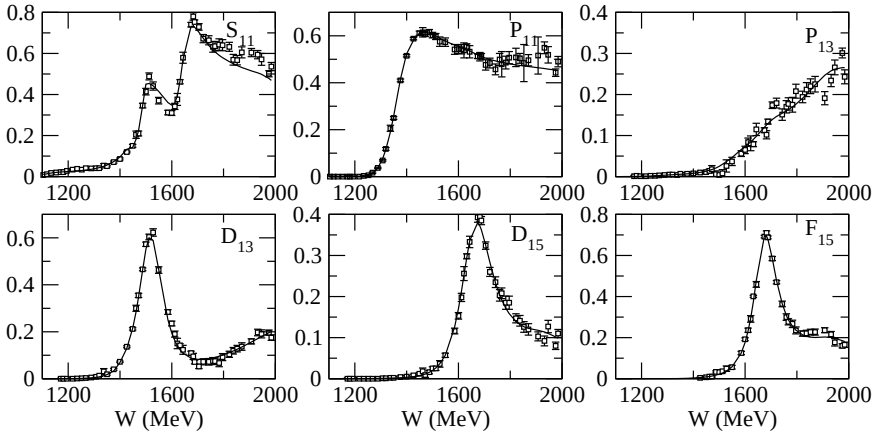

Figure 3: Imaginary part of $T_{\pi N,\pi N}$ for some isospin 1/2 partial waves compared to the SAID energy independent extraction.

polarization asymmetry is given in figures 4 and 5.

Our model is further checked by examining our predictions of the total cross sections σ^{tot} which can be calculated from the forward elastic scattering amplitudes by using the optical theorem.

The predicted σ^{tot} (solid curves) along with the resulting total elastic scattering cross sections σ^{el} compared with the data of $\pi^- p$ reaction are shown in Fig. 6. Clearly, the model can account for the data very well within the experimental errors. Equally good agreement with the data for $\pi^+ p$ reaction is achieved. In the right side of Fig. 6, we show how the contributions from each channel add up to get the total cross sections.

The contributions from $\pi\Delta$, ρN and σN intermediate states to the $\pi^- p \to \pi\pi N$ total cross sections calculated from our model can be seen in the right side of Fig. 6. These predictions remain to be verified by the future experiments. The existing $\pi N \to \pi\pi N$ data are not sufficient for extracting *model independently* the contributions from each unstable channel.

As mentioned above, the fit to πN elastic scattering can not determine well the bare $N^* \to \pi\Delta, \rho N, \sigma N$ parameters. Thus the results for these unstable particle channels must be refined by fitting the $\pi N \to \pi\pi N$ data, this is currently being pursued [9].

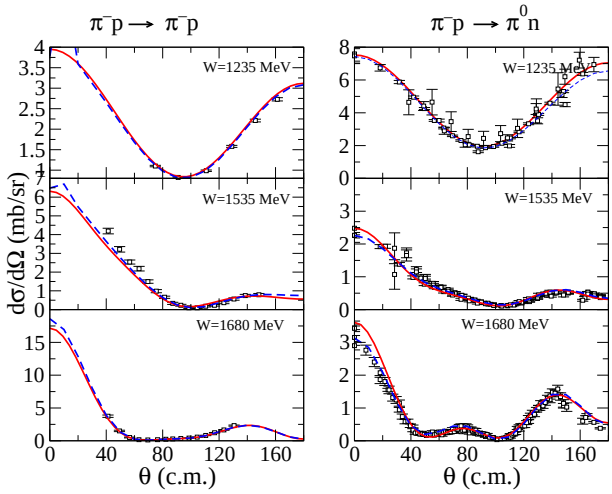

Figure 4: Differential cross section for several different center of mass energies. Solid red curve corresponds to our model while blue dashed lines correspond to the SP06 solution of SAID [7]. All data have been obtained through the SAID online applications. Ref. [11].

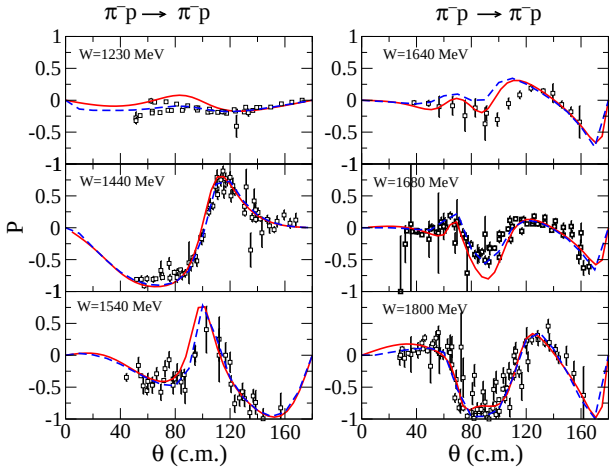

Figure 5: Target polarization asymmetry, P, for several different center of mass energies. Solid red curve corresponds to our model while blue dashed lines correspond to the SP06 solution of SAID [7]. All data have been obtained through the SAID online applications. Ref. [11].

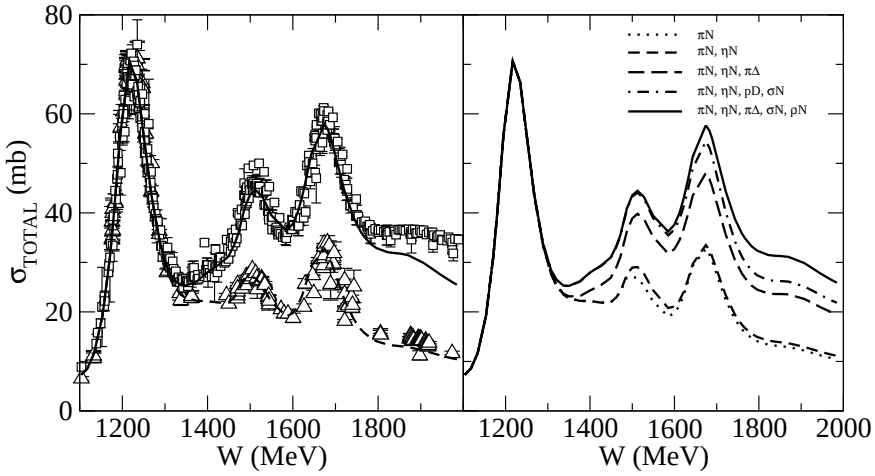

Figure 6: Left: The predicted total cross sections of the $\pi^- p \to X$ (solid curve) and $\pi^- p \to \pi^- p + \pi^0 n$ (dashed curve) reactions are compared with the data. Open squares are the data on $\pi^- p \to X$ from Ref. [10], open triangles are obtained by adding the $\pi^- p \to \pi^- p$ and $\pi^- p \to \pi^0 n$ data obtained from Ref. [10] and SAID database [11] respectively. Right: Show how the predicted contributions from each channel are added up to the predicted total cross sections of the $\pi^- p \to X$.

4 Photoproduction reactions

With the hadronic parameters determined in the previous fit to meson-baryon experimental data we proceed to analyze the extensive data base of π photoproduction. Here the only parameters that need to be determined are the bare $\gamma N \to N^*$ vertex interactions.

The strategy is to start with the bare helicity amplitudes of resonances at the values given by the PDG [10]. Then, we allow small variations with respect to those values and also in a preliminary step small variations of a selected set of non-resonant parameters. At the present stage we can only present preliminary results which are at the present time being further improved and will be reported elsewhere.

In figure 7 we present a comparison of the current model and the experimental differential cross section data for the reaction $\gamma p \to \pi^+ n$ at a fixed angle, $\theta = 90$ (deg). First, our main emphasis is put on understanding the region up to 1.6 GeV extending in that way previous works where only the Δ (1232) region was studied [4, 12, 13]. In figure 8 we depict angular distri-

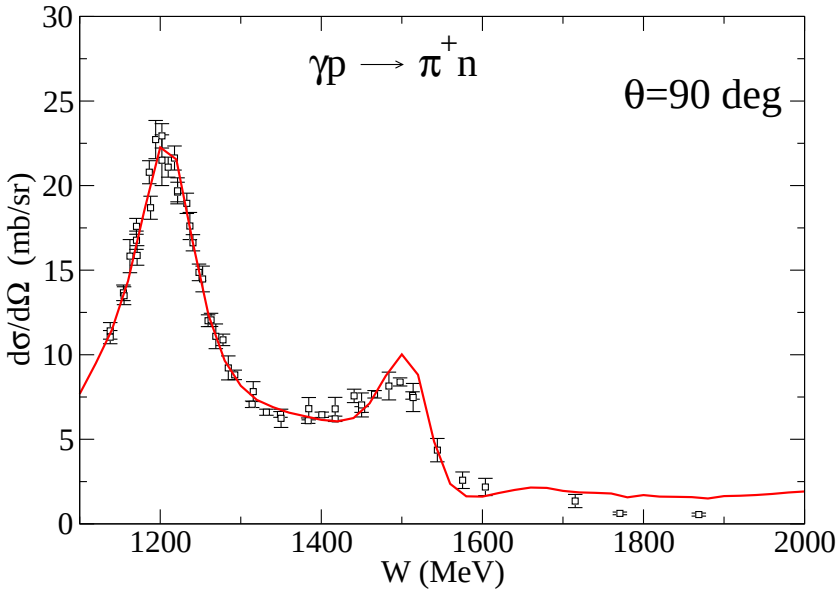

Figure 7: Differential cross section for the reaction $\gamma p \to \pi^+ n$ at $\theta = 90$ deg as function of the center of mass energy, W.

butions for both $\pi^+ n$ and $\pi^0 p$ photoproduction in the $\Delta(1232)$ region. The effect of intermediate meson-baryon states different from πN is also depict. The importance of multi-step processes is clear and confirms previous studies done in similar frameworks.

5 Future Developments

The model described in detail in Refs. [1,8] has already been used to study πN scattering and π photoproduction reactions as presented in this contribution. Being the main and most important interest of these studies the extraction and interpretation of baryon resonances by analyzing the extant photo and electro production experimental data we are now beginning to perform simultaneous studies of meson-baryon, single meson electro (photo)production [14] and two-meson photoproduction.

At the same time an important effort is being pursued to reliably extract meaningful resonance parameters from the coupled-channels formalism [15].

The simultaneous consideration of other meson-baryon channels, such as ωN [16] or kaon-hyperon channels is being pursued within the same frame-

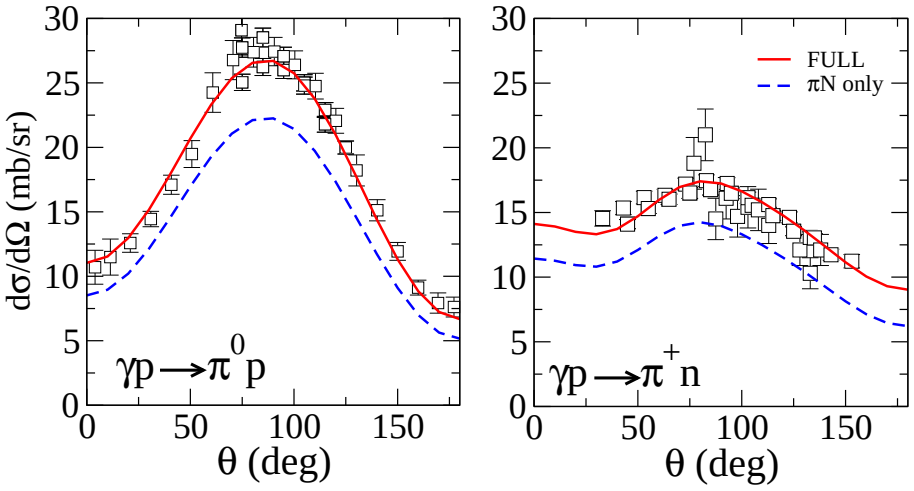

Figure 8: Differential cross section in the Δ region. The full line corresponds to the current full model, the dashed line only considers intermediate πN intermediate states in the photoproduction process.

work.

Acknowledgments

It is a pleasure to thank T.-S. H. Lee, A. Matsuyama and T. Sato who collaborated in everything presented here. I want to thank also the hospitality of the theory group at JLAB where part of this work was done. This work is partially supported by Grant No. FIS2005-03142 from MEC (Spain) and FEDER and European Hadron Physics Project RII3-CT-2004-506078. The computations were performed at NERSC (LBNL) and Barcelona Supercomputing Center (BSC/CNS) (Spain).

References

[1] A. Matsuyama, T. Sato, T.-S. H. Lee, *Phys. Rept.* **439**, 193 (2007).

[2] V. Burkert and T.-S. H. Lee, *Int. J. of Mod. Phys.* **E13**, 1035 (2004).

[3] T.-S. H. Lee and L.C. Smith, *J. Phys. G* **34**, 1 (2007).

[4] T. Sato and T.-S. H. Lee, *Phys. Rev. C* **54**, 2660 (1996).

[5] M. Kobayashi, T. Sato, and H. Ohtsubo, *Prog. Theor. Phys.* **98**, 927 (1997).

[6] Herman Feshbach, *Theoretical Nuclear Physics, Nuclear Reactions* (Wiley, New York, 1992)

[7] R.A. Arndt, I.I. Strakovsky, R.L. Workman, *Phys. Rev. C* **53**, 430 (1996); *Int. J. Mod. Phys.* **A18**, 449 (2003).

[8] B. Julia-Diaz, T.-S. H. Lee, A. Matsuyama, and T. Sato, *arXiv:0704.1615*. To appear in *Phys. Rev. C.*

[9] B. Julia-Diaz, H. Kamano, T.-S. H. Lee, A. Matsuyama, and T. Sato, in preparation.

[10] W. M. Yao *et al.* [Particle Data Group], *J. Phys. G* **33**, 1 (2006).

[11] CNS Data Analysis Center, GWU, **http://gwdac.phys.gwu.edu**.

[12] T. Sato and T.-S. H. Lee, *Phys. Rev. C* **63**, 055201 (2001).

[13] B. Julia-Diaz, T.-S. H. Lee, T. Sato and L. C. Smith, *Phys. Rev. C* **75**, 015205 (2007).

[14] B. Julia-Diaz, T.-S. H. Lee, A. Matsuyama, T. Sato, L.C. Smith in preparation.

[15] N. Suzuki, T. Sato and T.-S.H. Lee, in preparation.

[16] M.W. Paris, T. Sato and T.-S.H. Lee, in preparation.